3rd URSI AT-AP-RASC, Gran Canaria, 29 May – 3 June 2022

Transient Response for Slanted Gratings in Dispersion Medium

R. Ozaki*(1) and T. Yamasaki(1)
(1) College of Science and Technology, Nihon University

Abstract

In recent year, we have analyzed the transient scattering problem composed of dispersion media and rectangular air region by using a combination of the fast inversion of Laplace transform (FILT) method and the Fourier series expansion method (FSEM), and investigated an influence for several widths of the rectangular air region.
In this paper, we analyzed the transient response for slanted grating structure formed of periodically arrayed dispersion media and slanted air region by novel numerical techniques to utilizing the combination of the FILT, FSEM, and multilayer division method (MDM), and examined the influence for several slanted angle and width.

1. Introduction

Recently, the inverse scattering problem of the electromagnetic waves has been of interest in many fields of medicine and engineering. For example, there are such as imaging technology, remote sensing by micro or millimeter waves, and other radar signal processing. In particular, the ground penetrating radar (GPR) utilizing microwave band is well known as technology which can explore the target objects in the subsurface structure [1, 2]. And so, we are required to examine without destroying the target object in underground. Therefore, it is important to investigate the wave reflected from the scatterer such as conducting and dielectric geometries. However, in general, the permittivity of the underground structure is a function of frequency. Furthermore, in order to analyze the transient response with high accuracy, it is necessary to uniformly treat the complex dielectric constant of the dispersion property [3].
In recent papers, we have analyzed the transient scattering problem of periodically arrayed dispersion media with rectangular air region by using a combination of the Fourier series expansion method (FSEM) and the fast inversion of Laplace transform (FILT) method, and examined an effect of rectangular air region from resulting waveform by varying those widths [4].
In this paper, we analyze the transient response for slanted grating structure formed of periodically arrayed dispersion medium and slanted air region by novel numerical techniques to utilizing the combination of the FILT, FSEM, and multilayer division method (MDM). Numerical results are given for resulting waveform by varying various slanted angle and medium widths in TE case [5]-[7].

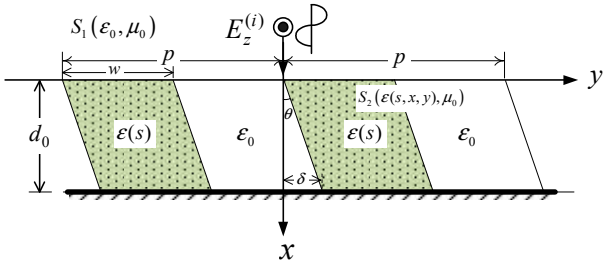

Figure 1. Structure and coordinate system for slanted grating formed by periodically arrayed dispersion medium and slanted air region.

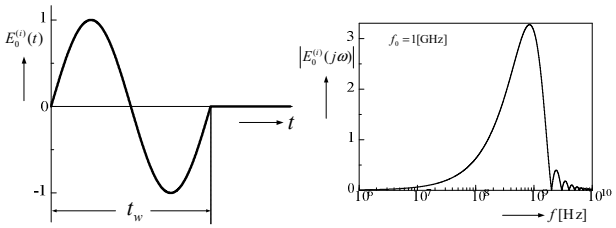

(a)Incident waveform (b)Spectrum

Figure 2. Incident pulse waveform and its spectrum (a)incident waveform, (b)spectrum.

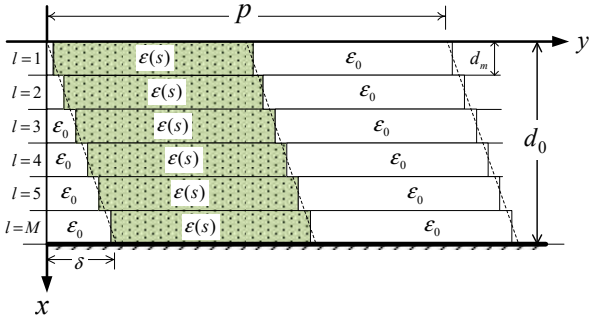

Figure 3. Example of multilayer division in one period for case of $M=6$.

2. Method of analysis

We discuss the slanted grating formed by periodically arrayed dispersion medium with slanted air region as shown in Fig.1. The region S_1 ($x<0$) is free space and the region S_2 ($0\le x\le d_0$) is slanted grating layer with

depth d_0 and the permittivity $\varepsilon(s,x,y)$ in complex frequency domain is a periodic function of *y*-direction with period p. Figure 1 is uniform in the *z*-direction. Here, the width of dispersion medium region is w, the slanted angle θ is defined as $\tan^{-1}(\delta/d_0)$ and also δ is the parameter of slanted width. The permeability is assumed to be μ_0 throughout. The time factor of the electromagnetic fields is exp(*st*) in complex frequency domain and is omitted in the field expression.

Next, we formulate the electromagnetic fields for the case of vertical incident plane wave with the electric field of only z component in complex frequency domain.

Firstly, the Laplace transform of Maxwell equation is used to derive the electromagnetic fields in regions S_1 and S_2. Therefore, the waveform of the incident pulse at $x=0$ is assumed to be a sine pulse as shown in Fig.2(a) in time domain and its image function can be expressed as

$$E_0^{(i)}(s)=\frac{\omega_0}{s^2+\omega_0^2}(1-e^{-st_w}), \tag{1}$$

where $\omega_0(:=2\pi/t_w)$ is an angular frequency, $t_w(:=1/f_0)$ is the pulse width and f_0 is the center frequency. The reflected waves can be expanded as the truncation mode number N_1 by using Floquet's theorem to obtain the following equation:

$$E_z^{(r)}(s,x,y)=\sum_{n=-N_1}^{N_1} R_n e^{k_1^{(n)}(s)x-i\frac{2n\pi}{p}y}, \tag{2}$$

$$H_y^{(r)}(s,x,y)=\frac{1}{s\mu_0}\frac{\partial E_z^{(r)}(s,x,y)}{\partial x}, \\ =\frac{1}{s\mu_0}\sum_{n=-N_1}^{N_1} R_n k_1^{(n)}(s) e^{k_1^{(n)}(s)x-i\frac{2n\pi}{p}y}, \tag{3}$$

$$k_1^{(n)}(s):=\sqrt{k_0^2(s)-(-i\,2n\pi/p)^2}, \tag{4}$$

$$k_0(s):=s\sqrt{\varepsilon_0\mu_0}=s/c_0, \tag{5}$$

where $k_0(s)$ is the wave number in free space, c_0 is the velocity of light, and $k_1^{(n)}(s)$ is the propagation constants in the *x*-direction. From the above, the electric fields of region S_1 can be expressed as sum of the incident and reflected waves as follows:

$$E_z^{(1)}(s,x,y)=E_0^{(i)}(s)e^{-k_0(s)x}+E_z^{(r)}(s,x,y), \tag{6}$$

By using the MDM, we are expressed the electromagnetic fields in slanted grating region S_2 ($0<x\le d_0$). Thus, the electromagnetic fields of the each thin layers as shown in Fig.3 can be expressed as solution to be satisfied wave equation by using the eigenvalue $h_\nu^{(l)}(s)$ and eigenvector $u_{\nu,n}^{(l)}$ found from eigenvalue equation as follows:

$$E_z^{(2,l)}(s,x,y)=\sum_{\nu=1}^{2N_1+1}\left[A_\nu^{(l)}e^{-h_\nu^{(l)}(s)\{x-(l-1)d_m\}} + B_\nu^{(l)}e^{h_\nu^{(l)}(s)\{x-ld_m\}}\right]\cdot f_{\nu,n}^{(l)}(y), \tag{7}$$

$$f_{\nu,n}^{(l)}(y):=\sum_{n=-N_1}^{N_1} u_{\nu,n}^{(l)} e^{-i\frac{2n\pi}{p}y},\ (1\le l\le M), \tag{8}$$

$$H_y^{(2,l)}(s,x,y)=\frac{1}{s\mu_0}\frac{\partial E_z^{(2,l)}(s,x,y)}{\partial x}, \tag{9}$$

where $A_\nu^{(l)}, B_\nu^{(l)}$ are unknown coefficients to be determined from boundary conditions. By the boundary conditions at $x=0$, $x=ld_m$ ($l=1\sim(M-1)$), and $x=d_0$, we will derive the relational equation of unknown coefficients.

Firstly, we can obtain the relational equation by matrix algebra from boundary conditions at $x=0$ and $x=d_0$ as follows:

$$\boldsymbol{Q}_1\boldsymbol{A}_\nu^{(1)}+\boldsymbol{Q}_2\boldsymbol{B}_\nu^{(1)}=\boldsymbol{E}_i, \tag{10}$$

$$\boldsymbol{Q}_3\boldsymbol{A}_\nu^{(M)}+\boldsymbol{Q}_4\boldsymbol{B}_\nu^{(M)}=\boldsymbol{0}, \tag{11}$$

where,

$\boldsymbol{Q}_\kappa:=[q_{\nu,n}^{(\kappa)}]$, $\kappa=1\sim4$,

$q_{\nu,n}^{(1)}:=(k_1^{(n)}(s)+h_\nu^{(1)}(s))u_{\nu,n}^{(1)}$, $-N_1\le n\le N_1$,

$q_{\nu,n}^{(2)}:=(k_1^{(n)}(s)-h_\nu^{(1)}(s))e^{-h_\nu^{(1)}(s)d_m}u_{\nu,n}^{(1)}$, $\nu=1\sim(2N_1+1)$,

$q_{\nu,n}^{(3)}:=e^{-h_\nu^{(M)}(s)d_m}u_{\nu,n}^{(M)}$, $q_{\nu,n}^{(4)}:=u_{\nu,n}^{(M)}$, $d_m:=d_0/M$,

$\boldsymbol{A}_\nu^{(\alpha)}:=[A_1^{(\alpha)},A_2^{(\alpha)},\cdots,A_{2N_1+1}^{(\alpha)}]^T$,

$\boldsymbol{B}_\nu^{(\alpha)}:=[B_1^{(\alpha)},B_2^{(\alpha)},\cdots,B_{2N_1+1}^{(\alpha)}]^T$, $\alpha=1 or M$,

$\boldsymbol{E}_i:=[0,\cdots,(k_0(s)+k_1^{(0)}(s)),\cdots,0]^T$.

Next, by using the boundary condition at $x=ld_m$, we can expand the relational equation of the unknown coefficients as following equations:

$$\begin{pmatrix}\boldsymbol{A}_\nu^{(1)}\\ \boldsymbol{B}_\nu^{(1)}\end{pmatrix}=\begin{pmatrix}\boldsymbol{G}_1^{(1)} & \boldsymbol{G}_2^{(1)}\\ \boldsymbol{G}_3^{(1)} & \boldsymbol{G}_4^{(1)}\end{pmatrix}\begin{pmatrix}\boldsymbol{G}_1^{(2)} & \boldsymbol{G}_2^{(2)}\\ \boldsymbol{G}_3^{(2)} & \boldsymbol{G}_4^{(2)}\end{pmatrix}\cdots\begin{pmatrix}\boldsymbol{G}_1^{(M-1)} & \boldsymbol{G}_2^{(M-1)}\\ \boldsymbol{G}_3^{(M-1)} & \boldsymbol{G}_4^{(M-1)}\end{pmatrix}\begin{pmatrix}\boldsymbol{A}_\nu^{(M)}\\ \boldsymbol{B}_\nu^{(M)}\end{pmatrix}, \\ =\begin{pmatrix}\boldsymbol{G}_1 & \boldsymbol{G}_2\\ \boldsymbol{G}_3 & \boldsymbol{G}_4\end{pmatrix}\begin{pmatrix}\boldsymbol{A}_\nu^{(M)}\\ \boldsymbol{B}_\nu^{(M)}\end{pmatrix}, \tag{12}$$

where,

$\boldsymbol{G}_\kappa^{(l)}:=[g_{\nu,n}^{(\kappa,l)}]$, $\kappa=1\sim4$, $l=1\sim(M-1)$,

$g_{\nu,n}^{(1,l)}:=[\Theta_{\nu,n}^{(l)}+\Theta_{\nu,n}^{(l)}h_\nu^{(l+1)}(s)/h_\nu^{(l)}(s)]e^{h_\nu^{(l)}(s)d_m}/2$,

$g_{\nu,n}^{(2,l)}:=[\Theta_{\nu,n}^{(l)}-\Theta_{\nu,n}^{(l)}h_\nu^{(l+1)}(s)/h_\nu^{(l)}(s)]e^{-\{h_\nu^{(l+1)}(s)-h_\nu^{(l)}(s)\}d_m}/2$,

$g_{\nu,n}^{(3,l)}:=[\Theta_{\nu,n}^{(l)}-\Theta_{\nu,n}^{(l)}h_\nu^{(l+1)}(s)/h_\nu^{(l)}(s)]/2$,

$g_{\nu,n}^{(4,l)}:=[\Theta_{\nu,n}^{(l)}+\Theta_{\nu,n}^{(l)}h_\nu^{(l+1)}(s)/h_\nu^{(l)}(s)]e^{-h_\nu^{(l+1)}(s)d_m}/2$,

$\boldsymbol{\Theta}_{\nu,n}^{(l)}:=[u_{\nu,n}^{(l)}]^{-1}\cdot[u_{\nu,n}^{(l+1)}]$, $\nu=1\sim(2N_1+1)$,

$-N_1\le n\le N_1$.

Therefore, from the Eqs.(10)-(12), we can obtain the matrix simultaneous equation for $\boldsymbol{A}_\nu^{(M)}$ as follows:

$$\boldsymbol{X}_t\cdot\boldsymbol{A}_\nu^{(M)}=\boldsymbol{E}_i, \tag{13}$$

where $\boldsymbol{X}_t$ is coefficient matrix defined by following equation:

$$\boldsymbol{X}_t:=[(\boldsymbol{Q}_1\boldsymbol{G}_1+\boldsymbol{Q}_2\boldsymbol{G}_3)-(\boldsymbol{Q}_1\boldsymbol{G}_2+\boldsymbol{Q}_2\boldsymbol{G}_4)\boldsymbol{Q}_4^{-1}\boldsymbol{Q}_3]. \tag{14}$$

We derive the other unknown coefficients $A_\nu^{(1)}$, $B_\nu^{(1)}$, $B_\nu^{(M)}$ from solution obtained by solving Eq.(14). Hence, we can find numerically the reflection coefficients R_n by using the unknown coefficients in complex frequency domain. The reflected electric and magnetic fields $E_z^{(r)}(s,x,y)$,

$H_y^{(r)}(s,x,y)$ in complex frequency domain obtained are transformed into the normalized time domain by using the following FILT method [8]:

$$E_z^{(r)}(T,X,Y) \coloneqq \frac{1}{2\pi i}\int_{\gamma-i\infty}^{\gamma+i\infty} E_z^{(r)}(S,X,Y)e^{ST}\,dS\,,$$

$$= \frac{e^a}{T}\left[\sum_{n=1}^{N-1} F_n - 2^{-(J+1)}\sum_{L=0}^{J} C_{JL}F_{N+L}\right], \qquad (15)$$

where,

$$F_n \coloneqq (-1)^n \,\mathrm{Im}\left[E_z^{(r)}(S,X,Y)\right],\ S \coloneqq \frac{a+i(n-0.5)\pi}{T},$$

$$C_{JJ}=1,\ C_{JL-1} \coloneqq C_{JL} + \frac{(J+1)!}{L!(J+1-L)!},$$

N is the truncation mode number of the FILT method, J is the number of terms in the Euler transformation, $S(\coloneqq st_w)$ is the normalized complex frequency, $T(\coloneqq t/t_w)$ is the normalized time, and $X(\coloneqq x/d_0)$, $Y(\coloneqq y/p)$ are the normalized coordinates.

3. Numerical analysis

Firstly, we employed the dispersion characteristics as following equation composed of the Sellmeier formula and loss term of water:

$$\frac{\varepsilon(s)}{\varepsilon_0} = 1+\sum_{j=1}^{3}\frac{\Omega_j^2}{s^2+g_j s+\omega_j^2}+\frac{\tau_0}{1+s\tau_1}, \qquad (16)$$

The parameters of Eq.(16) are given from Ref.[9]. In the following analysis, the parameters of numerical calculation were set as normalized depth $D_0(\coloneqq d_0/p)=0.2$, normalized period $P(\coloneqq p/(ct_w))=1$, $a=4$, $J=5$, $N=10$, $N_1=20$, $M=10$, $f_0=1$ GHz, an observation points $X=0$, $Y=0$, and dispersion characteristics with soil moisture 5%.

Figure 4 and 5 show the waveform of transient response for the reflection electric field $E_z^{(r)}(T)$ and magnetic field $H_y^{(r)}(T)$ by varying the normalized slanted width $\Delta(\coloneqq \delta/p)$ as condition of normalized medium width $W_p(\coloneqq w/p)=0.5$. From in Figs.4 and 5, we can see the following features:

(1-1)For the case of the reflection electric field in Fig.4, the effect of slanted width is seen clearly at $0.5 \le T \le 2.5$ as Δ increase. As this reason, we can consider as influence of the multiple reflection from slanted dispersion medium.

(1-2)The same effect appears in the case of the reflection magnetic field in Fig.5, but a large reflection response waveform is obtained as Δ increase.

Next, in order to examine the effects of Figs.4 and 5, we investigate if from the difference waveform due to the electric and magnetic fields.

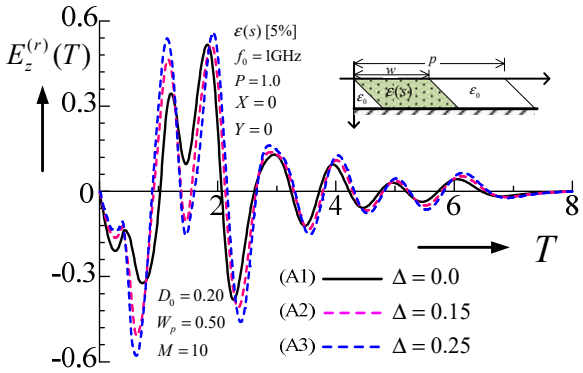

Figure 4. Waveform of reflected electric field for varying normalized slanted width.

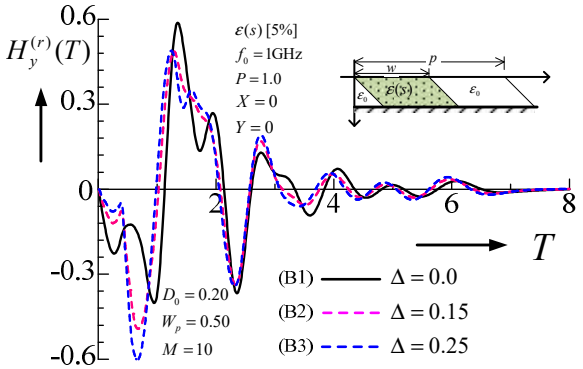

Figure 5. Waveform of reflected magnetic field for varying normalized slanted width.

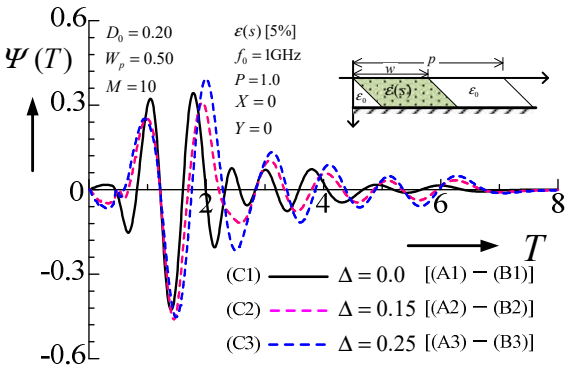

Figure 6. Differential waveform $\Psi(T)$ of the electric and magnetic fields for varying slanted widths. $\Psi(T)$ is the result of $E_z^{(r)}(T)-H_y^{(r)}(T)$.

Figure 6 shows the differential waveform $\Psi(T)$ for the results of $E_z^{(r)}(T)-H_y^{(r)}(T)$ under the conditions of Figs.4 and 5. From Fig.6, we can see the following features:

(2-1)We can see that the tendency of characteristics is seen phase delay and the amplitude large at $T \ge 1.5$ as Δ increase. As a one of this reason, we can think as influence by multiple reflections for slanted air region.

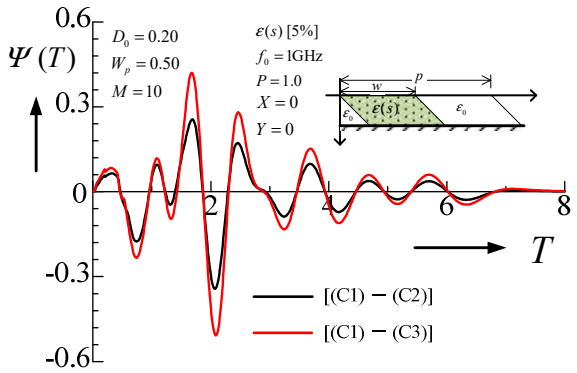

Figure 7. Differential waveform of Fig.6.

(2-2)We can consider that it can be extracted the influence of the slanted cavity by further taking the difference between results of C1 and C2 or C3. Finally, in order to confirm this effect of slanted cavity, we will examine the difference waveform obtained by using the results of C1, C2, and C3.

Figure 7 shows the differential waveform $\Psi(T)$ given by using the results of C1, C2, and C3. From Fig.7, we can see the following features:

(3-1)The phase of both results are the almost same, but we can see the amplitude of the difference response waveform becomes large proportional to the Δ.

(3-2)From above discussion (3-1), we can consider that the influence of the slanted cavity width can be identified by taking the responses amplitude for the difference waveform of the electric and magnetic fields.

4. Conclusion

In this paper, we analyzed the transient response of slanted gratings in dispersion medium by using a combination of FILT, FSEM, and MDM methods, and investigated an influence of slanted widths from resulting waveform. We will further investigate the influence of both the slanted air region and dispersion medium from transient response analysis in the future.

5. Acknowledgements

This research was partially supported by JSPS KAKENHI Grant Number JP21K04239.

6. References

1. R. Persico, “Introduction to ground penetrating radar Inverse Scattering and Data Processing,”, Wiley, 2013.

2. P. Shannuan and I. L. Al-Qadi, “Calibration of FDTD Simulation of GPR Signal for Asphalt Pavement Compaction Monitoring,”, IEEE Trans. Geosci. Remote Sens., vol.53, no.3, pp.1538-1548, 2015.

3. L. B. Felsen Ed., “Topics in Applied Physics: Transient Electromagnetic Fields,” , vol.16, Springer-Verlag, 1976.

4. R. Ozaki and T. Yamasaki, “Pulse Responses from Periodically Arrayed Dispersion Media with an Air Region,”, IEICE Trans. Electron., vol.E102-C, no.6, pp.479-486, 2019.

5. T. Yamasaki and H. Tanaka, “Scattering of electromagnetic waves by a dielectric grating with planar slanted-fringe,”, IEICE Trans. Electron., vol.E76-C, no.10, pp.1435-1442, 1993.

6. H. Tanaka, T. Yamasaki, and T. Hosono, “Propagation characteristics of dielectric waveguides with slanted grating structure,”, IEICE Trans. Electron., vol.E77-C, no.11, pp.1820-1827, 1994.

7. R. Ozaki and T. Yamasaki, “Numerical Analysis of Pulse Response for Slanted Grating Structure with an Air Regions in Dispersion Media by TE case,”, IEICE Trans. Electron., vol.E105-C, no.4, 2022.(to be Published)

8. T. Hosono, “Numerical Inversion of Laplace Transform and some Applications to Wave Optics,”, Radio Science, vol.16, no.6, pp.1015-1019, 1981.

9. R. Ozaki, N. Sugizaki, and T. Yamasaki, “Numerical Analysis of Pulse Responses in the Dispersion Media,”, IEICE Trans. Electron., vol.E97-C, no.1, pp.45-49, 2014.